Snell's law for the Schwarzschild black hole

X. H. Zheng[1,*] and J. X. Zheng[2]

[1]*Department of Physics, Queen's University of Belfast, Belfast BT7 1NN, United Kingdom*
[2]*Department of Electrical and Electronic Engineering, Imperial College London,
London SW7 2AZ, United Kingdom*

The Wheeler equation, for electromagnetic disturbances in a gravitational field, was found by Fiziev to have exact solutions both above and below the event horizon, in the form of waves propagating both inwardly and outwardly. This observation can be interpreted and verified from the optical point of view, entirely on the basis of the Schwarzschild metric for length contraction and time dilation, in order to derive a differential version of Snell's law for the Schwarzschild black hole. It reveals interesting physics, including the correct amount of light deflection by the Sun, internal and external Oppenheimer-Snyder cones of the black hole, properties of its phonon sphere and the conclusion that light rays are kept below the horizon by length contraction and time dilation rather than deflection.

I. INTRODUCTION

Electromagnetic fields in the Schwarzschild metric have been investigated for a long time [1–12] and Fiziev secured an unusual advance in 2006 [13]. With an explicit substitution he transformed the Wheeler equation [14] into Heun's equation [15] which is known to have exact solutions, both above and below the event horizon of a black hole, in the form of waves propagating both inwardly and outwardly. He presented a number of such solutions and commented on their eventual physical significance and some open problems [13].

The Wheeler equation was derived in 1955, from a system of fundamental equations for coupled electromagnetic and gravitational fields, to study strong electromagnetic disturbances capable of distorting spacetime to trap themselves [14]. Sometimes the Wheeler equation is referred to as the Regge-Wheeler equation probably because, in 1957, the two authors jointly published a paper on a related topic [16]. In the case of a black hole and weak electromagnetic disturbances the Wheeler equation assumes a specific form in the so-called tortoise coordinate in association with the Schwarzschild metric. With this specific Wheeler equation Fiziev applied his substitution and linked it to Heun's equation.

Heun's equation was studied by Karl Heun in the late 19th century and still is an active topic of contemporary investigation. It is a second-order ordinary differential equation with four singularities in its general form. By the process of confluence the number of singularities can be reduced (to three in the case of the Wheeler equation) for a rich variety of useful and important applications. Solutions to Heun's equation include local solutions (power series), Heun functions, Heun polynomials and path-multiplicative solutions [15]. The solutions Fiziev found are mostly local solutions, where a countable set exists below the event horizon, simultaneously finite at the horizon and center, and obviously square integrable. In his opinion, if these are proven to form a complete set in the corresponding functional space, they will present a natural basis of normal modes for a well-defined expansion of any small perturbation of the metric in the interior of the black hole [13].

The perspective of Fiziev amounts to a sophisticated scheme to analyze waves, essentially via Fourier expansion in terms of the so-called normal modes, which are solutions to the Wheeler equation, with a boundary value (zero for example) imposed upon the event horizon by some physics which, to the best of our knowledge, has not yet been identified.

Here we tackle the problem from the optical point of view so that, as long as light rays exist in the void below the event horizon, in addition to their presence above, it is sufficient for us to know length contraction and time dilation from the Schwarzschild metric to determine the speed of the waves in order to trace the rays, with no need to identify additional physics. The result is a differential version of Snell's law which, like its counterpart in classical optics, reveals interesting physics.

For example, above the event horizon, our version of Snell's law enables us to find the correct amount of light deflection by the Sun via straightforward evaluation. It enables us to define quantitatively the external Oppenheimer-Snyder cone, together with properties of the so-called phonon sphere, to determine whether or

*xhz@qub.ac.uk

not a ray launched above the event horizon can escape from the gravitational field. It also tells us clearly that, if incapable of escaping, the ray must encounter the event horizon at a right angle.

Below the event horizon, we find from our version of Snell's law the internal Oppenheimer-Snyder cone to determine the allowed angles for light rays to propagate in both the outward and inward directions. Historically Einstein started with optics to derive the general theory of relativity [17], adding length contraction and time dilation to the arsenal of optics as devices to manipulate light rays. We conclude that deflection, the traditional device in optics to manipulate light, on its own cannot retain light rays below the event horizon.

We arrange this article as follows. In Sec. II we explain the motions of light rays in a gravitational field. In Sec. III we specify relations between the speed of light and gravity. In Sec. IV we derive a differential version of Snell's law for black holes. In Sec. V we apply Snell's law to find the correct amount of light deflection by the Sun. In Secs. VI and VII we study analytical and numerical trajectories of the rays. In Sec. VIII we discuss the Wheeler equation. Brief discussions and conclusions are in Sec. IX.

II. HUYGENS PRINCIPLE AND GRAVITY

In 1678 the Dutch physicist Huygens proposed that every point to which a luminous disturbance reaches becomes a source of a spherical wavelet, and the sum of these wavelets determines the form of the luminous disturbance at any subsequent time [18]. He applied this principle to explain linear and spherical wave propagation, and to derive the laws of reflection and refraction. In 1911 Einstein applied the same principle to explain deflection of light rays in a gravitational field, and to outline the general theory of relativity [17]. In Fig. 1 we redraw the historic illustration by Einstein with some modifications. We follow Einstein to show how the wavelets emitted from two exemplary points on the first wave front, P_1 and P_2, expand and determine the second wave front. In addition we show how the same process repeats itself to determine the third front.

In Fig. 1 the wave fronts can be seen as the floors and roof of a two-level building, with the wavelets for pillars to support the first floor and roof. Einstein stated: "the velocity of light in the gravitational field is a function of the place" [17]. From now on we will refer to Einstein's "velocity of light" in the quotation as the speed of light seen by a distant observer, or the visual speed of light. We also will refer to the velocity of light seen by a local observer as the local speed of light, or simply the speed of light, which is a relativistic invariant. In the upper part of the figure gravity is uneven at P_1 and P_2 so that the building tilts towards P_2 where the visual speed of light is slower due to stronger gravity. In the lower part of Fig. 1 gravity is even at
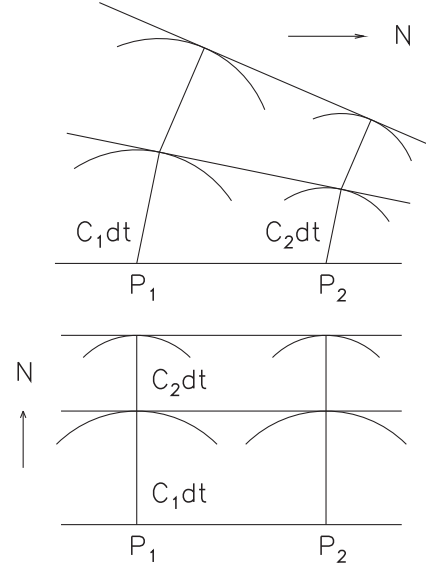

FIG. 1. Illustrations of the Huygens principle originally from Einstein, where P_1 and P_2 are centers on the first wave front to emit spherical wavelets whose envelope becomes the next front to emit further wavelets, C_1 and C_2 are visual speeds of light (as defined in Sec. II) which become slower the stronger the gravity, and dt is the differential time of wavelet expansion. The ray is launched either parallel to (upper part) or towards (lower part) the event horizon (location indicated by N).

P_1 and P_2 so that the building does not tilt but with its levels piled closer to each other the stronger the gravity.

Now we have a problem: what would happen if a ray were launched from below the event horizon to approach the horizon at a right angle, as is shown in the lower part of Fig. 1? It definitely will not make a U-turn and fall back to the center, because it is well known that the wavelets in the Huygens principle cannot propagate in the backward direction. From the optical point of view, what could stop the ray from escaping across the event horizon?

We will show that light rays launched outwardly from below the event horizon indeed encounter the horizon at right angles. They are kept below the horizon not by deflection but by length contraction and time dilation, which in our view are new devices in the arsenal of optics to manipulate light, capable of lending deflection a helping hand to impede and eventually stop the escaping rays on their outward trajectories.

III. VISUAL SPEED OF LIGHT AND GRAVITY

Above the event horizon the Schwarzschild metric can be written as

$$(ds)^2 = (d\ell')^2 - c^2(dt')^2, \qquad r > r_s \qquad (1)$$

where c is the local speed of light, or speed of light, invariant under all circumstances,

$$(d\ell')^2 = \left(1 - \frac{r_s}{r}\right)^{-1}(dr)^2 + r^2(d\Omega)^2,$$

$$(dt')^2 = \left(1 - \frac{r_s}{r}\right)(dt)^2 \qquad (2)$$

measure length contraction and time dilation, with r_s being the Schwarzschild radius, and $(d\Omega)^2 = (d\theta)^2 + \sin^2(\theta)(d\phi)^2$. We are reminded that the Schwarzschild metric is presented in the coordinate system (t, r, θ, ϕ) accommodating a distant observer. It is valid only in the presence of the factor $(1 - r_s/r)^{-1}$ for length contraction, and $1 - r_s/r$ for time dilation. It tells us $d\ell'/dt' = c$, because $ds = 0$ for light rays, that is the speed of light is invariant in the eyes of a local observer experiencing both length contraction and time dilation. But this is not true in the eyes of the distant observer. Letting

$$\cos^2(\alpha)(d\ell)^2 = (dr)^2,$$

$$\sin^2(\alpha)(d\ell)^2 = r^2(d\Omega)^2 \qquad (3)$$

where α is the angle of incidence made by the ray and the radial direction, explicitly specified as α_1 and α_2 at B and C in Fig. 2, we find from Eqs. (1) and (2)

$$\left(\frac{d\ell'}{dt'}\right)^2 = \frac{r^2}{(r - r_s)^2}\left[1 - \frac{r_s}{r}\sin^2(\alpha)\right]\left(\frac{d\ell}{dt}\right)^2 \qquad (4)$$

or $(d\ell'/dt')^2 = V^2(d\ell/dt)^2$ to relate the local and visual speed of light. We should take notice that in Eq. (4) $d\ell'$ and dt' are local measurements, whereas r, r_s, α and $d\ell$ are from the distant observer, comparable with say an object and its optical image. Consequently V can be compared with the refractive index that defines images in classical optics. Indeed Eq. (4) tells us clearly that, when $\alpha = 0$, we have $v = d\ell/dt = (1 - r/r_s)c$ which is the well-known formula for the visual speed of a ray in the radial direction of a Schwarzschild black hole from the eyes of the distant observer.

We follow the same procedure to investigate light rays below the event horizon. In this case the Schwarzschild metric is written as

$$-(ds)^2 = (d\ell')^2 - c^2(dt')^2, \qquad r < r_s \qquad (5)$$

where

$$(d\ell')^2 = \left(\frac{r_s}{r} - 1\right)^{-1}(dr)^2 - r^2(d\Omega)^2,$$

$$(dt')^2 = \left(\frac{r_s}{r} - 1\right)(dt)^2 \qquad (6)$$

which too leads to $d\ell'/dt' = c$ when $ds = 0$. Equations (2) and (6), like the Schwarzschild metric, are presented in the

coordinate system (t, r, θ, ϕ), valid only in the presence of the length contraction and time dilation factors. Equation (4) still applies but under the condition

$$\sin^2(\alpha) \leq \frac{r}{r_s} \qquad (7)$$

in order to avoid V, defined below Eq. (4), from becoming imaginary, a new issue arising from the term $-r^2(d\Omega)^2$ in Eq. (6).

To understand Eqs. (4) and (7) it is worth noting that Eqs. (2) and (6) are our choice, or ansatz, to test if we are correct to anticipate light rays below the event horizon. Our choice assumes consistency between Eqs. (1) and (5), true because they differ just by the sign of $(ds)^2$, which vanishes in the case of light rays. In addition our choice is evidently supported by the observation of Fiziev that the Wheeler equation has exact solutions both above and below the horizon [13]. In fact in the Wheeler equation the time factor, $\exp(i\omega t)$ (declared to be an ansatz by Fiziev), also is a choice to test if the equation has similar solutions both above and below the event horizon [13,14]. The test might fail, or become reduction to absurdity, in case the ansatz leads to a contradiction in general. Since Eq. (6) leads to a contradiction only when Eq. (7) is violated, not in general, we might be correct to expect light rays below the event horizon, provided we can find the physical reason for Eq. (7).

In the Schwarzschild metric length contraction takes place only in the r direction. Above the event horizon it has less of an effect in other directions due to the term $r^2(d\Omega)^2$ in Eq. (2). Below the event horizon, however, length contraction is always enhanced by the term $-r^2(d\Omega)^2$ in Eq. (6). When Eq. (7) has been violated, the enhancement to length contraction turns out to be so significant that $(d\ell')^2$ in Eq. (6) becomes negative, indicating the wavelets in the Huygens principle can no longer be in phase to direct their energy to form a thin pencil around a single direction, similar to what happens to the refractive ray when total reflection occurs. Indeed the criterion for total reflection in classical optics does bear a fair resemblance to Eq. (7).

Equation (7) defines a cone about the radial direction, with aperture $\to 0$ when $r \to 0$. In a landmark paper in 1939 Oppenheimer and Snyder revealed that, by the gravitational deflection of light, all energy emitted from the surface of a collapsing star will almost all be reduced to within a cone about the outward normal, of progressively shrinking aperture as the star contracts [19]. From now on we will refer to the cone defined in Eq. (7) as the internal Oppenheimer-Snyder cone, because it also is from gravitational deflection, located below the event horizon, with the aperture progressively shrinking with decreasing values of r, similar to what happens on the surface of a contracting star.

IV. SNELL'S LAW FOR BLACK HOLES

We apply Eq. (4) to specify the rule to determine the direction of light rays in the Schwarzschild metric. On account of the principle of phase matching we must have

$$V_1 \sin(\alpha_1) = V_2 \sin(\alpha_2 + \delta\phi) \qquad (8)$$

for the ray in Fig. 2. Here $V_1 = V(r_1, \alpha_1)$ and $V_2 = V(r_2, \alpha_2)$ are values of V defined in Eq. (4), α_1 and α_2 are ray angles of incidence against the outward normal, and $\delta\phi$ is the incremental angle made by r when it rotates to take the values r_1 and r_2. Equation (8) can be written as

$$V_1 \frac{\sin(\alpha_2 + \delta\phi) - \sin(\alpha_1)}{\alpha_2 + \delta\phi - \alpha_1} (\alpha_2 + \delta\phi - \alpha_1)$$
$$= -\frac{V_2 - V_1}{\delta\phi} \sin(\alpha_2 + \delta\phi)\delta\phi$$

which can readily be transformed into a differential equation. To this end we divide the above equation by $\delta\phi$ and let $\delta\phi \to 0$ so that $(\alpha_2 + \delta\phi - \alpha_1)/\delta\phi \to d\alpha/d\phi + 1$, assuming $\alpha_2 \to \alpha_1$ when $\delta\phi \to 0$. At the same time we find $\cos(\alpha_1)$ on the left-hand side of the above equation. We also find $dV/d\phi$ and $\sin(\alpha_1)$ on the right-hand side of the equation, assuming $V_2 \to V_1$ when $\delta\phi \to 0$. Letting $\alpha_1 = \alpha$ for generality, we find via simple rearrangement of the terms that

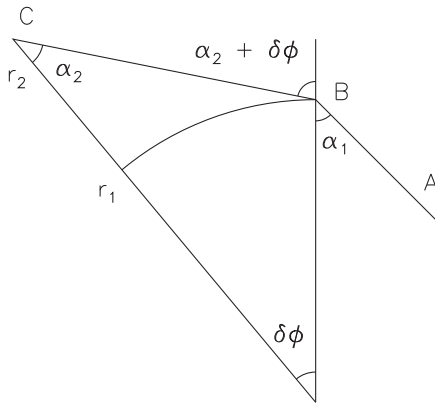$$\frac{d\alpha}{d\phi} = -1 - \frac{r}{V}\frac{dV}{dr}\frac{\tan(\alpha)dr}{rd\phi}$$

where

FIG. 2. Passage of a ray defined as $r(\phi)$ in the (r, ϕ) plane of the spherical coordinates, (r, ϕ, θ), with $r_1 = r(\phi_1)$, $r_2 = r(\phi_2)$, $\delta\phi = \phi_2 - \phi_1$. The ray is shown to start from A, and be deflected at B with an angle of incidence, α_1, and refraction, $\alpha_2 + \delta\phi$, both against the r direction. Eventually it reaches C with an angle of incidence, α_2, also measured against r. The visual speed of the ray is determined by V_1 or V_2 when $r < r_1$ or otherwise.

$$\frac{\tan(\alpha)dr}{rd\phi} = \lim_{\delta\phi \to 0} \frac{\tan(\alpha_2)(r_2 - r_1)}{r_1\delta\phi} = 1$$

from the geometry in Fig. 2, giving

$$\frac{d\alpha}{d\phi} = -1 - \frac{r}{V}\frac{dV}{dr}, \qquad \frac{dr}{d\phi} = r\cot(\alpha) \qquad (9)$$

as a differential version of Snell's law for Schwarzschild black holes. With the help of the expression of V in Eq. (4), and some rather involved algebra, we find

$$\left[1 - \frac{2r_s}{r}\sin^2(\alpha)\right]\frac{d\alpha}{d\phi} = -\left[1 - \frac{r_s}{2r}\sin^2(\alpha)\right]$$
$$+ \left[1 - \frac{r_s}{r}\sin^2(\alpha)\right]\frac{r_s}{r - r_s} \qquad (10)$$

to evaluate $d\alpha/d\phi$ in Eq. (9).

V. LIGHT DEFLECTION BY THE SUN

Letting $r_1 = 6.96 \times 10^8$ and $r_s = 2.95 \times 10^3$ be the radius and Schwarzschild radius of the Sun in meters respectively, we have $r_s/r < r_s/r_1 = 4.24 \times 10^{-6}$ for a ray passing the Sun at a grazing angle. Since in Eq. (4) the term $(r_s/r)\sin^2(\alpha)$ represents a high-order correction, due to inhomogeneous length contraction in different directions, we neglect similar terms in Eq. (10) (radial gravity approximation) and find

$$\frac{d\alpha}{d\phi} = -1 + \frac{r_s}{r - r_s} \qquad (11)$$

where the effect of gravitational deflection is represented by the last term on the right-hand side. To a very good approximation $r - r_s \simeq r_1/\cos(\phi)$ holds to give

$$\alpha = \int_{-0.5\pi}^{0.5\pi} \frac{r_s}{r - r_s} d\phi \simeq \frac{2r_s}{r_1} = 1.75 \text{ arc seconds} \qquad (12)$$

as the amount of light deflection by the Sun, consistent with the well-known astronomical observation.

VI. ANALYTICAL TRAJECTORIES: RADIAL GRAVITY APPROXIMATION

To illustrate the physics we integrate Eq. (11) analytically for simplicity and clarity. By using the second formula in Eq. (9) to eliminate $d\phi$ we find

$$\frac{r}{dr}\frac{d\sin(\alpha)}{\sin(\alpha)} = -1 + \frac{r_s}{r - r_s} \qquad (13)$$

which is a closed relationship between α and r ready to be integrated. The result is

$$\frac{r/r_s}{1 - r_s/r}\sin(\alpha) = \frac{r_0/r_s}{1 - r_s/r_0}\sin(\alpha_0) \qquad (14)$$

for trajectories of light rays in the radial gravity approximation, where r_0 and α_0 are the initial conditions of the ray. Letting r and r_s be the radius and Schwarzschild radius of the Earth for example, we have $r/r_s \simeq r_0/r_s = 7.18 \times 10^8$ and Eq. (14) tells us $\sin(\alpha) \simeq \sin(\alpha_0)$, that is a ray around us must travel along a straight path in its initial direction. If the ray is launched to ascend and pulled back by gravity afterwards, then $\alpha = \pi/2$ must occur at some stage, giving via Eq. (14)

$$\frac{r_s - r_0}{r_0^2}r^2 + \sin(\alpha_0)r - \sin(\alpha_0)r_s = 0 \qquad (15)$$

to determine the maximum value of r the ray can reach. Equation (15) has no real solution if

$$\sin(\alpha_0) \le 2\sqrt{\frac{r_s}{r_0} - \left(\frac{r_s}{r_0}\right)^2} \qquad (16)$$

which means the initial angle is too steep for the ray to be pulled back. Equation (16) can be compared with Eq. (7) and can be seen as an extended criteria for total reflection. From now on we will refer to the cone defined by Eq. (16) as the external Oppenheimer-Snyder cone, because the two authors discussed a similar cone above the surface of a collapsing star [19].

Equation (16) tells us that $\alpha_0 = 0$ when $r_0 = r_s$, that is, immediately above the event horizon, a ray still can defy gravity and escape if it is launched in the radial direction. On the other hand we have $\alpha_0 = \pi/2$ when $r_0 = 2r_s$ where lies the so-called phonon sphere [20] made from circular orbits of rays launched horizontally.

Data from Eq. (14) are ready to be presented graphically to illustrate the physics. All we have to do is find ϕ from the second equation in Eq. (9) with a simple numerical procedure. To this end we need ϕ_0, in addition to r_0 and α_0, for the initial conditions to launch the rays. Above the event horizon in Fig. 3 we launch rays at $r_0 = 2r_s$ and $\phi_0 = 0.25\pi$ (northeast direction) with $0.05 \le \alpha_0 \le 0.48\pi$ to descend and ascend in the clockwise and counterclockwise directions respectively. The ascending rays are traced until $r = 2.5r_s$ whereas the descending rays are traced to encounter the event horizon ($r \simeq r_s$ with $\alpha = 0$). Afterwards the rays are shown to continue their journey to illustrate their straight trajectories ($\alpha \equiv 0$) until $r = 0.5r_s$.

We also launch rays below the event horizon at $r_0 = 0.5r_s$ and $\phi_0 = 1.25\pi$ (southwest direction) with $0.05 \le \alpha_0 \le 0.48\pi$ to ascend in counterclockwise directions. The rays are traced to encounter the event horizon ($r \simeq r_s$ with $\alpha = 0$) and continue their journey along straight lines ($\alpha \equiv 0$) until $r = 2.5r_s$. We are reminded that $r = r_s$ is a singular point where α in Eq. (14) has no definition. Each of
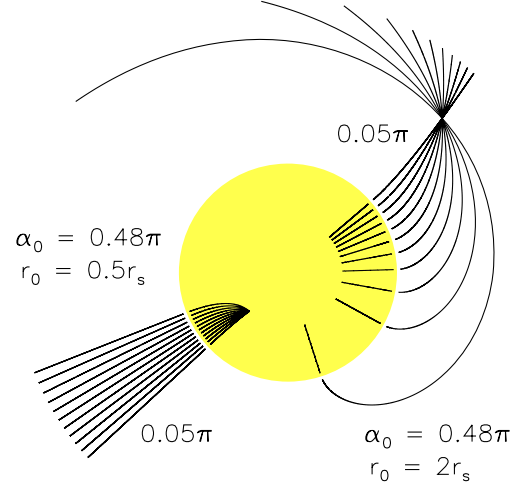

FIG. 3. Event horizon (interior shaded, radius $= r_s$) and analytic trajectories of rays in the radial gravity approximation from Eq. (14) and detailed discussion in Sec. VI. The rays are launched at $r_0 = 0.5$ or $2r_s$ with $0.05 \le \alpha_0 \le 0.48\pi$ until $r \sim r_s$. Afterwards the rays are illustrated to continue their journeys along straight lines, leaving a schematic gap behind indicating length contraction and time dilation.

the trajectories in Fig. 3 is made from two pieces separated by a gap to indicate infinite length contraction and time dilation.

VII. NUMERICAL TRAJECTORIES

To solve Eq. (10) we use the second equation in Eq. (9) to replace $d\phi$ with dr and apply the following numerical scheme:

$$\frac{u_{n+1}}{u_n} = 1 + \frac{\Delta\xi_n}{\xi_n - 2u_n^2}\left[\frac{2 - \xi_n}{\xi_n - 1}\right. $$
$$\left. + \left(\frac{3}{2\xi_n} - \frac{1}{\xi_n - 1}\right)u_n^2\right] \qquad (17)$$

where $u_n = \sin(\alpha_n)$, $\xi_n = r_n/r_s$, $\Delta\xi_n = \xi_{n+1} - \xi_n$, $n = 0, 1, 2, \ldots$, iteratively for rays above the event horizon, with the initial condition $\xi_0 = 2$ and $\phi_0 = 0.25\pi$, $0.05 \le \alpha_0 \le 0.3\pi$, and we let the ray ascend until $\xi = 2.5$, or descend until $\xi = 1 + \Delta\xi$, that is one numerical step above the event horizon. Afterwards we let the rays continue their journeys along straight trajectories until $\xi = 0.5$. We also apply Eq. (17) with the initial condition $\xi_0 = 0.5$ and $\phi_0 = 1.25\pi$, $0.05 \le \alpha_0 \le 0.16\pi$, and let the ray ascend until $\xi = 1 - \Delta\xi$, that is just one numerical step short below the event horizon. Afterwards we let the rays continue their journeys along straight trajectories until $\xi = 2.5$.

We evaluate Eq. (17) numerically with a first-order Runge-Kutta procedure written in house, always with 8000 steps when ξ varies between 0.5 and 2.5. We use the analytical solution in Eq. (14) as a reference to test the
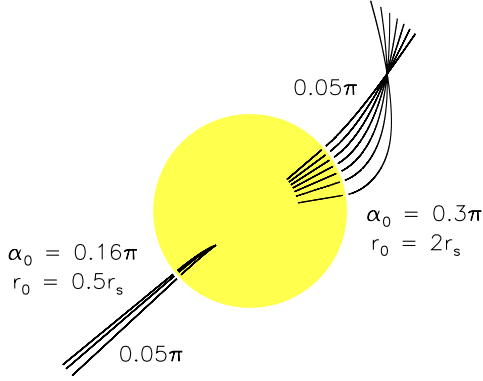
FIG. 4. Numerical trajectories of light rays from Eq. (17) and the detailed discussion in Sec. VII, with the same conventions as in Fig. 3, with the schematic gaps indicating infinite length contraction and time dilation in particular.

accuracy of the outcome of Eq. (17), with terms in $\sin^2(\alpha)$ removed from Eq. (10). We find that, over the range of ξ, the rms deviation in α is 1.15×10^{-4} on average when $\xi_0 = 0.5$ and 1.38×10^{-4} when $\xi_0 = 2$.

Our numerical trajectories from Eq. (17) are shown graphically in Fig. 4 ready to be compared with the analytical trajectories in Fig. 3. We find that, if we do not assume $\sin(\alpha) = 0$ for the radial gravity approximation, then we have to let $\alpha \leq 0.16\pi$ to restrict the initial incidence when the ray is launched at $\xi = 0.5$. The reason apparently lies in the internal Oppenheimer cone in Eq. (7) demanding $\alpha < 0.25\pi$ when $\xi = 0.5$. Above the event horizon we find we have to let $\alpha \leq 0.3\pi$ initially when the ray is launched at $\xi = 2$.

It is remarkable that, in Fig. 3, the ray launched with $r_0 = 2r_s$ and $\alpha_0 = 0.48\pi$ follows a nearly circular trajectory to orbit the event horizon. Furthermore, with $r_0 = 2r_s$ and $\alpha_0 = \pi/2$, we can balance Eq. (14) with $r \equiv 2r_0$ and $\alpha \equiv \pi/2$, which represents a perfect circular trajectory. However it is clear from Fig. 4 that, numerically, we cannot launch a ray to follow this trajectory. The reason lies in that, if we let $\sin^2(\alpha) = 1$ in Eq. (10), Eq. (13) will be replaced by

$$\frac{r}{dr}\frac{d\sin(\alpha)}{\sin(\alpha)} = -1 + \frac{r_s}{r - r_s} + \frac{r_s}{r - 2r_s}$$

for the transverse gravity approximation. It tells us $r \equiv 2r_s$ and $\alpha \equiv \pi/2$ definitely cannot be a solution to Eq. (10). The phonon sphere, specified in Sec. IV as made from circular rays at $r = 2r_s$ in the radial gravity approximation, cannot actually accommodate rays. It is interesting that, according to Nitta *et al.*, phonon orbits become unstable inside the phonon sphere [20].

VIII. WHEELER EQUATION

For the Schwarzschild metric and weak electromagnetic waves, with a negligible effect on spacetime curvature, the Wheeler equation assumes the form

$$\frac{d^2R}{dx^2} + \left[k^2 - \frac{L(L+1)}{r^2}e^\nu\right]R = 0 \qquad (18)$$

where $k = \omega/c$, ω is the circular frequency of the waves, L is the angular momentum, $e^\nu = 1 - r_s/r$ and $x = r + r_s \ln|r/r_s - 1|$ is the so-called tortoise coordinate [13]. If we add $3(r_s/r^3)e^\nu$ to the terms in the square brackets in Eq. (18) then we find the Regge-Wheeler equation for gravitational waves which, unlike the Wheeler equation, is perturbational and approximate [16].

Equation (18) is reduced to the Riccati-Bessel equation in flat spacetime, where $r_s \to 0$, $x \to r$ and $e^\nu \to 1$. If we let $R(r) = rZ(r)$ then Eq. (18) is further reduced to the standard spherical Bessel equation in $Z(r)$ and its first- and second-order derivatives in r [21]. In curved spacetime, however, it becomes very challenging to study Eq. (18), partly due to the simultaneous presence of both x and r. Fiziev found that Eq. (18) can be transformed into Heun's equation, with an explicit transform to remove x. He also found a number of exact solutions, mostly in the form of power series [13]. Now the challenge lies in understanding the physical implications of these solutions. For example Fiziev was not certain if a complete set can be found in a functional space to present a natural basis of normal modes for an expansion of the solution to Eq. (18) below the event horizon [13].

It is interesting that when $L = 0$ for electromagnetic disturbances without angular momentum, that is light rays propagating in the radial direction, the presence of r in Eq. (18) is automatically removed, and the equation is reduced to the Helmholtz equation, with a simple solution in the tortoise coordinate:

$$R(x) \propto \exp(i\omega t)\exp(-ikx) \qquad (19)$$

of which the real part is evaluated and shown in Fig. 5. It represents a harmonic wave propagating from $r = 0$ to ∞. Clearly we are justified to expect the void below the event horizon being filled with electromagnetic disturbances, that serves as the premise of our analysis.

In Eq. (19) we have $\omega t - kx = \text{const}$ for the location of a wave front, giving $\omega dt - kdx = \omega dt - kdr/(1 - r_s/r) = 0$, or $dr/dt = (1 - r_s/r)c$ as the speed of the wave. Letting $\alpha = 0$ in Eqs. (2) and (3) we also find $dr/dt = d\ell/dt = (1 - r_s/r)d\ell'/dt' = (1 - r_s/r)c$. Apparently solutions to the Wheeler equation can be identified as light rays in our black hole optics, at least in the radial direction, for the very reason that solutions to the Maxwell equation were identified as light rays for the first time in history.

In Eq. (19) the wave propagates outwardly, on account of the term $\exp(-ikx)$. The wave can also propagate inwardly, because we can replace $\exp(-ikx)$ with $\exp(ikx)$. This endorses our understanding that gravity cannot force a ray to make a U-turn and pull it back to the center, if the ray is launched outwardly towards the event horizon at a right
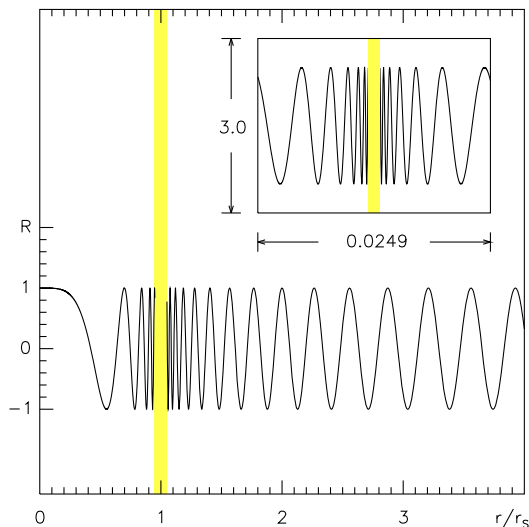
FIG. 5. Real part of the solution to the Wheeler equation ($L = 0$, $k = 12.57/r_s$) in Eq. (18) shown as a function of r. A section of the solution, over a shaded range of 0.0249 in r/r_s in the main frame, is shown in the inset for clarity. A section of the solution in the inset is also shaded for clarity. There can be an infinite number of such zoom-in procedures, like a Russian doll with infinite layers. No definite boundary value can be imposed on the event horizon for the Fourier expansion over $[0, r_s]$.

angle. It must be time dilation and length contraction that impede and eventually stop the escaping ray on its outward trajectory.

The effect of length contraction is clearly appreciable from Fig. 5. The real part of $R(r)$ oscillates, with the pitch growing progressively higher as $r \to r_s$ indicating that the wave fronts of $R(r)$ are squeezed tighter the closer the distance from the event horizon. Indeed, in the lower part of Fig. 1, the wave fronts from the Huygens principle are squeezed tighter towards the event horizon.

In Fig. 5 we have to shade sections of r close to the event horizon to hide high pitches for clarity, indicating that $R(r)$ has no definite value at $r = r_s$ (that is $x = \infty$). Therefore it may be difficult to find normal modes (solutions to the Wheeler equation with a definite boundary value at $r = r_s$ due to some physics) for a well-defined expansion of electromagnetic disturbances in the interior of the black hole [13].

IX. CONCLUSIONS

The theory for the gravitational and electromagnetic fields is represented in an elegant set of compact equations, namely the Einstein-Maxwell equations [1–12], or the Wheeler equation coupled with the Schwarzschild metric when spherical symmetry is assumed [14]. With an explicit substitution Fiziev transformed the Wheeler equation into

Heun's equation which is known to have exact solutions both above and below the event horizon, in the form of spherical waves propagating both inwardly and outwardly [13]. Therefore the void below the event horizon may not be empty but filled with electromagnetic disturbances (light rays) constantly trying to cross the horizon from below and escape.

To pull back or to slow down to a standstill? That is the question when the task is to prevent a ray from crossing a certain barrier. It turns out that, from the optical point of view, light rays may not be kept below the event horizon of a black hole by deflection, which cannot force the rays to make a U-turn and fall back when they are propagating towards the horizon to escape. It must be length contraction and time dilation that lend deflection a helping hand and slow the escaping rays to a standstill.

The optical point of view is in accordance with Einstein's vision with respect to light rays in a gravitational field, in terms of the Huygens principle, when he outlined his plan to develop the general theory of relativity [17]. It is immediately clear from his vision that deflection alone cannot stop light rays from escaping across the event horizon, because the wavelets in the Huygens principle cannot propagate in the backward direction. His vision also accommodates the possibility that light rays may be slowed down to a standstill in a strong gravitational field, although at that time the concept of a black hole had not yet been envisaged.

Oppenheimer and Snyder listed three reasons to explain why a collapsing star may close itself off from any communication with a distant observer, apart from via its gravitational field. Two of these, the Doppler effect and gravitational redshift, are devices from general relativity due to length contraction and time dilation. The remaining reason, concerning the aperture of the external Oppenheimer-Snyder cone in Sec. VI, is due to gravitational deflection [19]. It certainly helps to stop light rays from escaping, but may be compromised by the tendency of the light rays from below the event horizon to encounter the horizon at right angles.

Our black hole optics interprets and verifies the observation of Fiziev that the Wheeler equation has exact solutions both above and below the event horizon, in the form of waves propagating in both the outward and inward directions. Fiziev looks forward to identifying some physics, to impose a boundary condition upon the event horizon, that would enable him to find a natural basis of normal modes for a well-defined expansion of any small perturbation of the metric in the interior of the black hole [13]. Our black hole optics could become a useful alternative to help tackle this problem, because it is entirely based on the Schwarzschild metric, with no need for additional physics.

[1] W. B. Bonnor, Static magnetic fields in general relativity Proc. Phys. Soc. London Sect. A **67,** 225 (1954).

[2] D. Lovelock, A spherically symmetric solution of the Maxwell-Einstein equations, Commun. Math. Phys. **5,** 257 (1967).

[3] A. Papapetrou, Dipole electromagnetic radiation in a Schwarzschild space: The wavetail to order m/r, J. Phys. A **8,** 313 (1975).

[4] B. Linet, Dipole field solution of Maxwell's equations in the Schwarzschild metric, J. Phys. A **8,** 328 (1975).

[5] A. Bachelot, Scattering by black-hole for electromagnetic fields, in *Inverse Methods in Action*, edited by P. C. Sabatier (Springer, Berlin, 1990).

[6] A. Bachelot, Gravitational scattering of electromagnetic field by Schwarzschild black-hole, Ann. Inst. Henri Poincaré **54,** 261 (1991), http://www.numdam.org/item?id= AIHPA_1991__54_3_261_0.

[7] Ts. I. Gutsunaev and C. L. Ehl'Sgol'Ts, A new class of solutions of the magnetostatic Einstein-Maxwell equations, Zh. Eksp. Teor. Fiz. **104,** 2257 (1993), https://ui.adsabs .harvard.edu/abs/1993ZhETF.104.2257G/abstract.

[8] Y. Choquet-Bruhat1, P. T. Chruściel, and J. Loizelet, Global solutions of the EinsteinMaxwell equations in higher dimensions, Classical Quantum Gravity **23,** 7383 (2006).

[9] J. A. V. Kroon, The Maxwell field on the Schwarzschild spacetime: Behaviour near spatial infinity, Proc. R. Soc. A **463,** 2609 (2007).

[10] P. Blue, Decay of the Maxwell field on the Schwarzschild manifold, J. Hyperbolic Differ. Equations **5,** 807 (2008).

[11] E. M. Ovsiyuk, On solutions of Maxwell equations in the space-time of Schwarzschild black hole, Nonlinear Phenom. Complex Syst. **15,** 84 (2012), https://inspirehep.net/literature/ 1219506.

[12] P. G. S. Fernandes, C. A. R. Herdeiro, A. M. Pombo, E. Radu, and N. Sanchis-Gual, Spontaneous scalarisation of charged black holes: Coupling dependence and dynamical features, Classical Quantum Gravity **36,** 134002 (2019); **37,** 049501(C) (2020).

[13] P. P. Fiziev, Exact solutions of Regge-Wheeler equation and quasi-normal modes of compact objects, Classical Quantum Gravity **23,** 2447 (2006).

[14] J. A. Wheeler, Geons, Phys. Rev. **97,** 511 (1955).

[15] *Heun's Differential Equations*, edited by A. Ronveaux (Oxford University Press, Oxford, 1995).

[16] T. Regge and J. A. Wheeler, Stability of a Schwarzschild singularity, Phys. Rev. **108,** 1063 (1957).

[17] A. Einstein, Über den Einfluss der Schwerkraft auf die Ausbreitung des Lichtes, Ann. Phys. (Berlin) **340,** 898 (1911); English translation in *The Principle of Relativity* (Dover, New York, 1952).

[18] C. Huygens, *Treatise on Light* (MacMillan, London, 1912).

[19] J. R. Oppenheimer and H. Snyder, On continued gravitational contraction, Phys. Rev. **56,** 455 (1939).

[20] D. Nitta, T. Chiba, and N. Sugiyama, Shadows of colliding black holes, Phys. Rev. D **84,** 063008 (2011).

[21] M. Abramowitz and A. Stegun *Handbook of Mathematical Functions* (Dover, New York, 1972).